

A Fractal Space-filling Complex Network

D. J. B. Soares^{1,4}, J. Ribeiro Filho^{1,2}, A. A. Moreira¹, D. A. Moreira³, and G. Corso^{3,4}

¹ Departamento de Física, Universidade Federal
do Ceará, 60451-970 Fortaleza, CE, Brazil

² Curso de Matemática, Universidade Estadual
Vale do Acaraú 62040-370, Sobral, CE, Brazil

³ Departamento de Física Teórica e Experimental,
Universidade Federal do Rio Grande do Norte,

Campus Universitário, 59078 970 Natal, RN, Brazil and

⁴ Departamento de Biofísica e Farmacologia, Centro de Biociências,
Universidade Federal do Rio Grande do Norte,
Campus Universitário 59072 970, Natal, RN, Brazil

(Dated: November 7, 2018)

Abstract

We study in this work the properties of the Q_{mf} network which is constructed from an anisotropic partition of the square, the multifractal tiling. This tiling is build using a single parameter ρ , in the limit of $\rho \rightarrow 1$ the tiling degenerates into the square lattice that is associated with a regular network. The Q_{mf} network is a space-filling network with the following characteristics: it shows a power-law distribution of connectivity for $k > 7$ and it has an high clustering coefficient when compared with a random network associated. In addition the Q_{mf} network satisfy the relation $N \propto \ell^{d_f}$ where ℓ is a typical length of the network (the average minimal distance) and N the network size. We call d_f the fractal dimension of the network. In the limit case of $\rho \rightarrow 1$ we have $d_f \rightarrow 2$.

PACS numbers: 89.75.Da, 89.75.Hc, 61.43.Hv

Keywords: networks, fractals, space-filling, multifractal tiling, small-world

I - INTRODUCTION

The last years have seen an increasing interest in network studies in physics [1, 2]. Despite graph theory have been a research topic of mathematics and science of computation, the physicists have driven their attention to networks that show distribution of connectivity, $P(k)$, following a power law and that present small world effect: $\ell \propto \ln N$, for ℓ a typical network distance and N the size of the network. A recent article [3] points the difficulty to put together these two aspects in a common broad scale-free framework, it means, a fractal paradigm. In fact, a real fractal should have $N \propto \ell^{d_f}$ for d_f the fractal dimension, and not a logarithm dependence between N and ℓ . In this work we present a network that have the following characteristics: it is fractal, $N \propto \ell^{d_f}$, it is scale-free $P(k) \propto k^{-\gamma}$ for a large range of k , and it is complex in the sense of having large clustering coefficient. The scaling relation $N \propto \ell^d$ is trivially fulfilled for regular lattices where d is an integer, the topologic dimension of the space. The complex fractal network we explore in this paper has a non integer d_f .

Recently networks embedded in metric spaces have been investigated in the literature [4] because of the large applications of networks that effectively occupy a volume in 3-dimensions. In addition, motived by microprocessors design space-filling networks [5] have been studied. We cite these new trends in networks because the distinguished network we analyze in this paper is embedded in a metric space and furthermore it is space filling. In fact our network has a geometrical inspiration, it comes from a partition of the square. Indeed this network is originated from a singular tiling that has the additional property of being a multifractal partition of the square [6].

We follow the previous literature [6, 7, 8, 9, 10] and call this object the multifractal tiling, Q_{mf} . The Q_{mf} tiling was developed in the context of modeling transport and percolation in heterogeneous porous media. In fact, a broad set of irregular and heterogeneous systems are model in the literature using a multifractal approach. We cite systems in geology [11, 12], atmospheric science [13] and chemistry [14]. Oil reservoirs are complex anisotropic structures whose treatment have been challenged science and technique because of its non trivial geometry. Inspired in the description of oil reservoirs it was developed [6] the Q_{mf} tiling. In reference [7] an exhaustive study of the percolation threshold of Q_{mf} was performed, in [8] a random version of Q_{mf} was created, in [9] some of its percolation critical exponents were found, and in [10] a numerical study of its coordination number is done.

In this work we explore the network properties of the Q_{mf} , it means its topology, the study of the connections (neighborhood) among the cells of the tiling. The paper is organized as follows. In section 2 we describe in some detail the process of construction of the Q_{mf} tiling and show its more important properties. In section 3 we show the main results concerning the properties of the network: the distribution of connectivity, the scaling of the the average minimal distance between two sites and the clustering

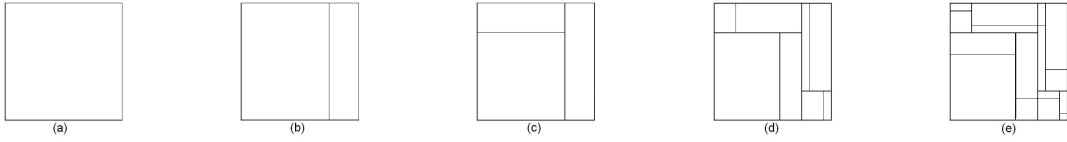


FIG. 1: The first five steps in the construction in the multifractal tiling Q_{mf} for $(s, r) = (1, 3)$.

coefficient. Finally in section 4 we present our conclusions, discuss the main implications of our results and compare the properties of the Q_{mf} network with other networks in the literature.

II - THE MULTIFRACTAL OBJECT

The multifractal tiling is a peculiar partition of the square. It is interesting to think about the Q_{mf} tiling in contrast to the square lattice. The square lattice can be constructed using the following algorithm: take a square and cut it symmetrically with horizontal and vertical lines. This procedure produces four square cells. Repeat this procedure n times inside each new block and you have finally a square lattice with 2^n cells. The Q_{mf} object is generated in a similar way as the square lattice above described, but instead of using a symmetric partition we perform horizontal and vertical sections following a given ratio.

In Fig. 1 we exemplify the five initial steps of the construction of the multifractal for the parameter $\rho = 1/3$, or $(s, r) = (1, 3)$. In 1 (a) we show, $n = 0$, the initial square that by convenience we assume of size $L = 1$. In (b), $n = 1$, a vertical cut is performed and two rectangles are formed. We call this a $(s, r) = (1, 3)$ object because the square is divided in 4 parts such that 1 part stays at one side and 3 parts at the other side. In (c), $n = 2$, two horizontal lines are drawn using the same section rate as before. At this level the initial square generates four rectangular blocks. Using as the area unit a square of size $\epsilon = 1/(s+r)$, the largest block has area r^2 , there are two blocks of areas rs and the smallest block has area s^2 . In (d) and (e), $n = 3$ and $n = 4$, respectively, the same procedure is repeated inside the initial four blocks. In reference [15] it is explored the group of eight possibilities of cutting a square lattice with a given ratio. In this work, as in other papers about Q_{mf} [6, 7, 8, 9, 10], it is followed the recipe of Fig. 1.

We remark that the number of blocks at step n is 2^n . These blocks do not have all the same area, we call the subsets of blocks of same area by a k -set. It is easy to check that the block area distribution follows a binomial distribution and the number of k -sets

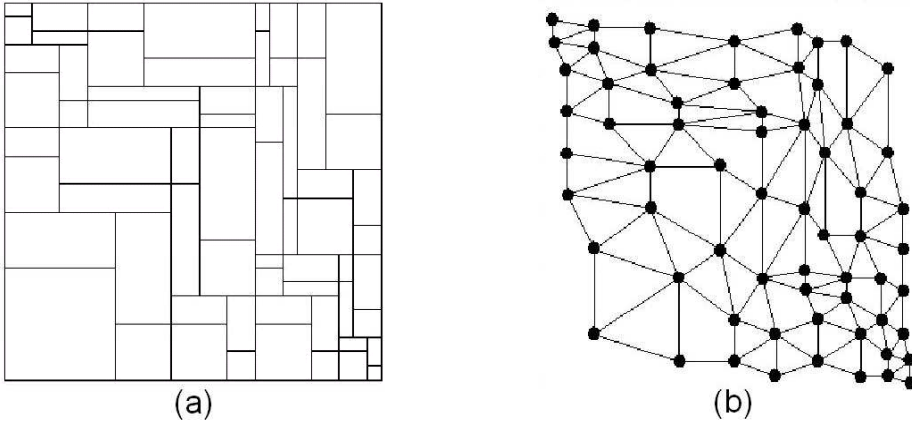


FIG. 2: A Q_{mf} multifractal tiling and a Q_{mf} network, for $\rho = 1/2$ and $n = 6$. In (a) the original tiling and in (b) the corresponding network.

is $k = n + 1$. This fact implies that the Q_{mf} has the remarkable property: in the limit of $n \rightarrow \infty$ the area of its forming blocks follows a multifractal distribution [6]. The spectrum of fractal distributions comes from a box counting reasoning:

$$D_X = \lim_{\epsilon \rightarrow 0} \frac{\log N(X)}{\log (1/\epsilon)} \quad (1)$$

for $N(X)$ the number of unitary cells of size length ϵ that cover the set of blocks of a given area X . Once the initial square is partitioned n times, the size of the unitary cell is $\epsilon = 1/(s+r)^n$. For each k -set the total area of blocks (using ϵ area units) is done by:

$$N_k = C_n^k s^k r^{(n-k)}, \quad (2)$$

where C_n^k is the binomial coefficient that express the number of elements k -type, and $s^k r^{(n-k)}$ is the area of each element of this set. We put together all these elements to have the fractal dimension of each k -set:

$$D_k = \lim_{\epsilon \rightarrow 0} \frac{\log N_k}{\log(1/\epsilon)} = \lim_{n \rightarrow \infty} \frac{\log(C_n^k s^k r^{(n-k)}))}{\log(s+r)^n}. \quad (3)$$

This distribution show a concave shape with a maximum at $k = \rho n$. The case $r = s = 1$ is degenerated. In this situation the subsets of the lattice are composed uniquely by square cells of the same area. Therefore the tiling is formed by a single subset of dimension 2.

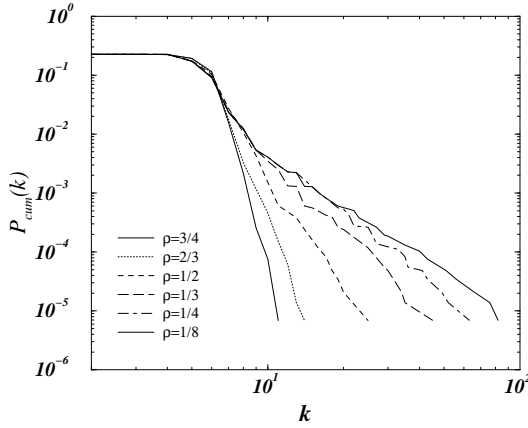


FIG. 3: The cumulative degree distribution for several values of ρ and $N = 2^{16}$. For $k > 7$ the distributions approaches a power-law form. The exponent γ controlling the decay of the distributions decreases in the limit of $\rho \rightarrow 0$, the full set of exponents is show in Table I.

In Fig. 2 (a) it is shown an example of Q_{mf} construction for $(s, r) = (1, 2)$ and $n = 6$. In Fig. 2 (b) we build a network corresponding to this tiling. The nodes of the network are the 2^n blocks of the Q_{mf} and the vertices are established according to a neighborhood criterium. These last figures offer a glimpse of the metric heterogeneity and the topology of the multifractal. In the next section we explore in detail the network properties of this class of objects.

III - RESULTS

We start the analysis of the properties of the Q_{mf} network discussing its distribution of connectivity, $P(k)$. In Fig. 3 we show the cumulative sum of $P(k)$ versus k for several values of ρ as indicated in the figure. The option for the cumulative sum instead of $P(k)$ itself is due to the strong fluctuation of the data. Fig. 3 confirms the results of a previous work [10]. For low k , typically $k < 7$, the curve suggests an exponential behavior and above this threshold the network depicts a scale-free behavior. The values of the exponents γ of the power-law $P(k) \propto k^{-\gamma}$ are indicated in Table I for several ρ , trivially the values of γ are estimated from the slopes of the curve of the cumulative sum decreased by one. The exponent γ goes to an asymptotic limit for large N [10]. We observe that in the limit of $\rho \rightarrow 1$ the Q_{mf} tiling gets more symmetric and at $\rho = 1$ the Q_{mf} degenerates into the square lattice. For the regular square lattice $P(k)$ is a delta of Dirac centered at $k = 4$ and the cumulative sum a step function. Fig. 3 corroborates this idea, the skewed curves in the $\rho \rightarrow 1$ limit anticipate the phase transition at $\rho = 1$.

We explore the distance characterization of the Q_{mf} network in Fig. 4 where we display the behavior of the average shortest distance for all couple of distinct vertices of the network, ℓ , versus network size, N . The simulation is performed for some values

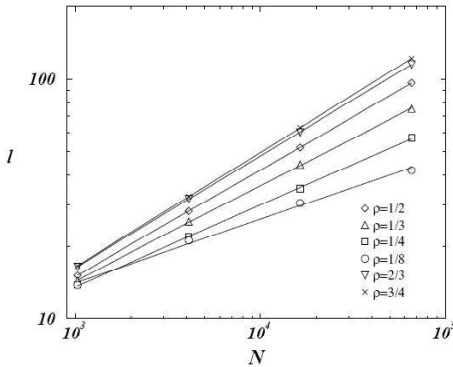


FIG. 4: In (a) it is displayed the average distance ℓ as a function of N for several values of ρ .

of ρ as indicated in the figure. For all ρ examined the data show a power-law behavior $N \propto \ell^{d_f}$. We find $2 < d_f < 4$, the full set of d_f is shown in Table I. Two limit cases are interesting. The limit $\rho \rightarrow 1$, which corresponds to the square lattice, has $d_f \rightarrow 2$ as it is expected in a bidimensional space. The opposit limit $\rho \rightarrow 0$, which is associated with very anisotropic structures, shows large d_f . We cannot affirm that 4 is an asymptotic threshold, further numerical investigation should test this hypothesis. We remark that the Q_{mf} network does not follow a small world relationship $\ell \propto \ln N$ that is common to most of power-law and random like networks.

An analysis of the clustering coefficient, C , versus network size, N , is shown in Fig. 5. The general view of this figure points to a stable behavior of C in the limit of large N . The dispersion of C among ρ is not large, the numerics show $C = 0.37 \pm 0.01$. Smaller values of ρ , however, show a significant larger C . The discussion about C is intriguing once we compare the numerical values of C with the clustering coefficient of a random network associated to the Q_{mf} network. An associated random network is defined as a network with the same N and $\langle k \rangle$ of the original network (we do not compare our results with a random network with a same $P(k)$ because such random network would alterate the space filling characteristics that we are interested in). For a random network $C = \langle k \rangle / N$, in the case of our network: $\langle k \rangle$ is a constant number smaller than 6 and N a number that can grow without limit. As a consequence the associated random

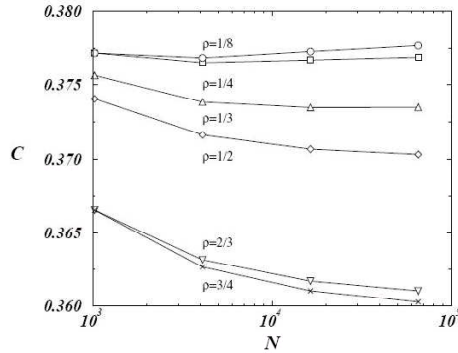


FIG. 5: In the clustering coefficient C as function of N for the same set of values of ρ of the previous figure.

network has $C \rightarrow 0$ in the limit $N \rightarrow \infty$. Therefore the Q_{mf} network has a C that is infinitely larger than the clustering coefficient of the associated random network. Because of the high C and the power-law behavior of distribution of connectivity we call the Q_{mf} network a complex network.

In Table I it is shown some parameters related to the Q_{mf} network for several values of ρ . Most of these data was already commented in the text. We focus now on the average connectivity $\langle k \rangle$ of the network. For all ρ studied we have $\langle k \rangle \sim 5.43$ which characterizes a sparse network. This is not surprising, since there is a result in topology that shows that for two dimensions the average coordination number of a tiling cannot exceed 6. The average connectivity confirms Fig. 3 where we can see that the majority of vertices are situated in the range: $4 \leq k \leq 6$. Otherwise we note that most of interesting results concerning the distribution of connectivity, in special the power-law behavior, are satisfied only in the range $k > 7$. Indeed, the Q_{mf} network, as most of complex networks, also have hubs that determine the distinguished characteristics of the network.

TABLE I: The average quantities: clustering coefficient, C , minimal distance, ℓ , and connectivity, $\langle k \rangle$; the slope γ of the distribution of connectivity and the fractal dimension d_f . The data corresponding to the average parameters are estimated for $N = 2^{16}$.

ρ	(3, 4)	(2, 3)	(1, 2)	(1, 3)	(1, 4)	(1, 8)
C	0.3603	0.3610	0.3703	0.3735	0.3769	0.3777
ℓ	122.02	115.26	96.43	75.12	57.12	41.70
$\langle k \rangle$	5.4357	5.4357	5.4338	5.4275	5.4357	5.4357
γ	16.6	11.1	6.4	4.2	3.4	2.9
d_f	2.09	2.14	2.25	2.52	2.94	3.79

IV - CONCLUSION

In this work we explore some properties of a space filling network that come from a multifractal partition of the square lattice, the Q_{mf} network. An analysis of the distribution of the connectivity, $P(k)$, assures that the Q_{mf} network shows a power-law tail that is more accentuated as increases the anisotropy of the underlying Q_{mf} tiling. Roughly the power-law tail of $P(k)$ starts at $k \sim 7$. We remark that there is no regular lattice in 2 dimensions with $k > 6$ and typical Voronoi lattices have an exponential small number of vertices in this range. In addition the Q_{mf} network has a clustering coefficient that approaches a constant, $C = 0.37 \pm 0.01$, that does not depend on N . This fact is in contrast to random networks that (for a constant $\langle k \rangle$) have $C \propto N^{-1}$. Because the value of C is much larger than the value of C of the associated random network we call the Q_{mf} network a complex network.

The most interesting aspect of the Q_{mf} network concerns its fractal behavior. For the average minimal path ℓ we observe that $N \propto \ell^{d_f}$ for the fractal dimension, d_f . The simulations show that $2 < d_f < 4$. The lower limit correspond to the case $\rho = 1$ where the multifractal tiling degenerates into the square lattice. In this situation the slope γ (from the power law $P(k) \propto k^{-\gamma}$) increases dramatically, this situation corresponds to the $P(k)$ of the square lattice that is of the form of a Delta of Dirac. The opposite limit, $\rho = 0$, corresponding to very anisotropic tilings, presents comparatively small values of γ .

We point that, diversly from [3], the Q_{mf} network shows an actual fractal behavior $N \propto \ell^{d_f}$ that is obtained without any renormalization artefact. In the reference [3] a ingenious procedure is used to calculate two fractal dimensions d_B and d_f . The first dimension depends on a suitable embedding in a metric space and a box counting methodology. The second is based on network distance and a mass (number of vertices) inside a given

radios. In our case, we have calculated d_f in the standard way, the box-counting, however, depends on the methodology we use to make the embedding of the Q_{mf} object. The simplest embedding is the Q_{mf} lattice itself that is a 2-dimensional object and as a result $d_B = 2$. Note that the multifractal property of Q_{mf} appears when we consider the subsets of blocks of same area, if we disregard the area set a bidimensional tiling assumes the trivial topologic dimension, $d_f = 2$.

The Q_{mf} tiling is indeed a remarkable mathematical object, from a metric perspective it is a multifractal: it is formed by a denumerable quantity of sets of different areas each one with a given fractal dimension. In a topologic perspective the connections among the vertices (the cells of the tiling) form a fractal network. We remark that regular networks (generated from lattices for instance) and the Bethe tree satisfy the criterium $N \propto \ell^d$, but these structures are regular. For the best knowledge of the authors the Q_{mf} network is the only case of a true fractal, scale-free and with high clustering coefficient.

Acknowledgments

The authors gratefully acknowledge the financial support of Conselho Nacional de Desenvolvimento Científico e Tecnológico (CNPq)-Brazil, FINEP and Programa PET-SESU/MEC. D. J. B. S. Thanks to D. R. de Paula.

- [1] R. Albert and A-L Barabási, Rev. Mod. Phy. **74**, 47 (2002).
- [2] S. H. Strogatz, Nature, **410**, 268 (2001).
- [3] C. Song, S. Havlin and H. A. Makse, Nature, **433** 392 (2005).
- [4] Danyel J. B. Soares, Constantino Tsallis, A. M. Mariz and L. R. da Silva, Europhys. Lett., **70**, pp 70-76 (2005).
- [5] J. S. Andrade,Jr, H. J. Hermann, R. F. S Andrade, and L. R. da Silva, Phys. Rev. Lett. **94**, 018702 (2005).
- [6] G. Corso, J. E. Freitas, L. S. Lucena, and R. F. Soares, Phys. Rev. E. **69**, 066135 (2004).
- [7] L. S. Lucena, J. E. Freitas, G. Corso, and R. F. Soares, Brazilian Journal of Physics **33**, 637 (2003).
- [8] M. G. Pereira, G. Corso, L. S. Lucena, and J. E. Freitas Chaos, Solitons and Fractals, **23**, 1105 (2004).
- [9] M. G. Pereira, G. Corso, L. S. Lucena, and J. E. Freitas, International Journal of Modern Physics C, **16** 317 (2005).
- [10] G. Corso, J. E. Freitas and L. S. Lucena, Physica A, **342** , 214 (2004).
- [11] R. H. Riedi, *Multifractals and wavelets: a potential tool in Geophysics*, Proceedings of the 68th SEG Meeting, New Orleans, Louisiana, USA, (1998).
- [12] F. Herrmann, *A Scaling Medium Representation, a Discussion on Well-logs, Fractals and*

Waves. PhD Thesis, Delft University of Technology, (1997).

- [13] J. Muller Annales Geophysicae - Atmospheres Hydrospheres and Space Sciences **11**, (6): 525-531 (1993).
- [14] H. E. Stanley and P. Meakin, Nature **355**, 405 (1988).
- [15] G. Corso and L. S. Lucena, Physica A (to appear) (2005).